The Mechanism of Single-Walled Carbon Nanotube Growth and Chirality Selection Induced by Carbon Atom and Dimer Addition

Qiang Wang,[†,‡] Man-Fai Ng,[‡] Shuo-Wang Yang,[‡,*] Yanhui Yang,[†] and Yuan Chen[†,*]

[†]School of Chemical and Biomedical Engineering, Nanyang Technological University, 62 Nanyang Drive, Singapore 637459, Singapore, and [‡]Institute of High Performance Computing, 1 Fusionopolis Way, no. 16-16 Connexis, Singapore 138632, Singapore

ABSTRACT On the basis of abounding density function calculations, a mechanism is proposed to explain single-walled carbon nanotube (SWCNT) growth and chirality selection induced by single C atom and C_2 dimer addition under catalyst-free conditions. Two competitive reaction paths, chirality change induced by single C atom and nanotube growth through C_2 dimer addition, are identified. The structures of the intermediates and transition states along the potential energy surfaces during the formation of near-armchair (6,5), (7,5), (8,5), and (9,5) caps initiated from the armchair carbon cap (5,5) are elucidated in detail. The results show that the direct adsorptions of C atom or C_2 dimer on growing carbon caps have no energy barrier. Moreover, the incorporations of adsorbed C atom or C_2 dimer display low energy barriers, indicating SWCNT growth and chirality change are thermodynamically and kinetically feasible under catalyst-free growth conditions. In addition, the results also highlight that the concentrations of C atoms and C_2 dimers in the experimental environment would play a critical role in the chiral-selective SWCNT synthesis. Potential opportunities exist in achieving the (*n*,*m*) selective growth by delivering single C atom or C_2 dimers at different ratios during different reaction stages.

KEYWORDS: single-walled carbon nanotube · growth · chirality · mechanism · carbon dimer addition

The physical and chemical properties of single-walled carbon nanotubes (SWCNTs) depend on their unique chiral structures, the direction in which a graphene sheet is rolled into a tube, specified by a chiral index (*n*,*m*).[1,2] Chiral-selective growth of SWCNTs is essential for their nanoscale assembly and technological applications. Intensive experimental[3−12] and theoretical[13−19] efforts have been dedicated to achieve the SWCNT chirality control. Experimental results have shown that various growth parameters, such as catalysts,[3,4,11,20] carbon precursors,[5,7−9] and substrates,[5,10,12] can influence the (*n*,*m*) selectivity.

The initial theoretical explanations on the (*n*,*m*) selectivity were mainly based on the carbon cap structural stability and the cap formation energies.[4,21] In particular, Balbuena *et al*. extended the cap structure stability to the (*n*,*m*) dependent carbon cap aromaticity and reactivity.[15,16] Because metal nanoparticles have been considered as an indispensable component in SWCNT growth, the interaction between carbon caps and metal nanoparticles was soon taken into consideration. Reich *et al*. proposed that particular (*n*,*m*) caps can be favored by their epitaxial relationship to the solid metal catalyst surface,[13,14] which implied the possibility of (*n*,*m*) chirality control through matching a SWCNT cap with a specific local crystalline lattice on metal surfaces. Reich *et al*. also suggested that the (*n*,*m*) selectivity is solely determined at the initial cap nucleation stage.[13,14] Balbuena *et al*. further investigated the interaction between carbon caps and small metal clusters, evidencing that the interaction strengths are different among (*n*,*m*) species.[17−19] Ding *et al*. noticed that strong adhesions between SWCNTs and the catalyst particles are necessary to support the nanotube growth. Also, the energy between dissociating SWCNT and metal catalyst particle may be (*n*,*m*) dependent.[22] They proposed that the (*n*,*m*) selective growth is possible if metallic alloys with different adhesion strengths are used.[22]

However, despite intensive experimental[23,24] and theoretical studies,[25−29] the details of carbon cap formations and their interactions with metal nanoparticles remain unclear. Moreover, some studies showed that the chirality of SWCNTs can be further changed during the growth on metal surfaces.[30,31] Ding *et al*. proposed a dislocation growth mechanism, in which nanotube growth rate is proportional to the chiral angle of a tube, suggesting (*n*,*m*) selectivity may be determined by

*Address correspondence to chenyuan@ntu.edu.sg; yangsw@ihpc.a-star.edu.sg.

Received for review December 4, 2009 and accepted January 12, 2010.

Published online January 27, 2010. 10.1021/nn901761u

nanotube growth rate.[32] A recent experimental study demonstrated that a growing nanotube is rotating, which supports this dislocation growth mechanism.[33]

Several recent experiments open up a new front for SWCNT synthesis by using nonmetal nanoparticles: oxides, such as SiO_2,[34−36] and zirconia[37] or dielectric materials, such as diamond.[38] It has been speculated that nonmetal nanoparticles may also catalyze SWCNT growth by aiding hydrocarbon decomposition and carbon cap assembly.[34,37] Nevertheless, the mechanism behind SWCNT growth on nonmetal nanoparticles is still unclear at this point.

Carbon species, such as single C atom and C_2 dimer, can be generated from decomposition of gaseous carbon precursors or evaporation of solid carbon sources. The direct interaction between carbon species and growing carbon nanotube structures is common in various SWCNT synthesis processes. An intriguing perspective is whether such direct interactions can induce (*n*,*m*) selectivity, especially under catalyst-free conditions. If SWCNT chirality can be manipulated through exposing small carbon caps to different carbon species, this may provide an additional tool toward (*n*,*m*) selective growth without worrying about the complex interactions between carbon caps and nanoparticles. As such, a detailed atomic level understanding of how do the caps evolve upon interacting with carbon species is essential in the quest for chirality-controlled growth. To address this, precise *ab initio* calculations of potential energy surfaces (PESs) and activation energies of various reaction paths are required.

In the current context, we uncover a mechanism for aforementioned SWCNT growth and chirality selection induced by single C atom and C_2 dimer addition based on abounding density function theory (DFT) calculation results. The armchair carbon cap (5,5) is selected as a starting point because some high chiral angle SWCNTs of (6,5), (7,5), (8,5), and (9,5) can be evolved from it. This family of high chiral angle tubes is most commonly found in chiral-selective SWCNT synthesis.[3,7,20] We present both singlet and triplet PESs of single C atom and C_2 dimers reacting with the caps (*n*,5) where (n = 5, 6, 7, 8, and 9), and the structures of the intermediates and transition states in each growth step. Finally, we propose the possible roles of nanoparticles in SWCNT synthesis and feasible means to achieve the chirality controlled SWCNT growth.

RESULTS

All optimized chiral caps are depicted in Figure 1 and the relative energies at different spin states are given in Table 1. It is found that the ground spin states of the caps are different. For example, the ground state of the cap (5,5) is singlet which is more stable than its triplet and quintet states by 0.56 and 1.13 eV, respectively. While, the ground states of the caps (6,5), (7,5), and (8,5) are triplet, and their energies are 0.56, 0.53, and 0.46 eV lower than their quintet states, respectively. Uniquely, the cap (9,5) has a quintet ground state, and its energy is lower than its triplet, septet, and singlet states by 0.53, 0.78, and 3.36 eV, respectively. The high spin multiplicity (triplet or quintet) found for the near-armchair (*n*,5) caps where (n = 6, 7, 8, and 9) suggests that those caps have higher possibility to react with carbon species with unpaired electron states, such as C_2 dimers.[17]

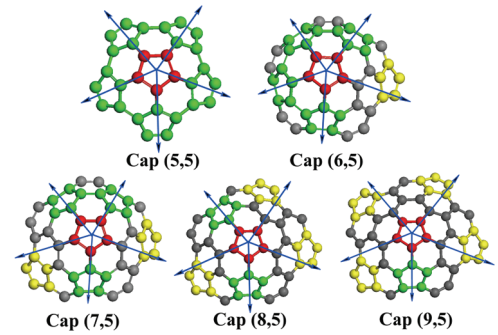

Figure 1. Geometric structures of selected caps with several chiralities fulfill the isolated pentagon rule.[39,40] The arrows denote the location of five pentagons for the cap (5,5) and the direction for moving pentagons outward.

To compare the stabilities of different caps, the energies *per* C atom relative to the cap (5,5) are listed in Table 2. The energies of the near-armchair caps (*n*,5) where (n = 6, 7, 8, and 9) are lower than that of the armchair cap (5,5) within the range of 0.31−0.36 eV *per* C atom. This agrees with the previous works by Balbuena *et al*. that the near-armchair caps are more stable as compared with the armchair caps.[15−17] Furthermore, the energy *per* C atom increases monotonically as the chiral angle decreases from the near-armchair cap (6,5) to (9,5), indicating that the near-armchair caps with larger chiral angles are more stable. It has been generally speculated that a stable cap is more likely leading to the continuous growth to be nanotubes.[4,13−19,21] However, the complex interaction between the carbon caps and nanoparticles make it tremendously difficult for researchers to either theoretically elucidate the SWCNT growth processes[25,26] or experimentally achieve highly (*n*,*m*) selective growth. In this study, we focused on the evolution of carbon caps upon reacting with carbon species under catalyst-free conditions.

There are two possible competitive reaction pathways at the initial growth stage starting from the (5,5) cap: single C atom incorporation which results in chirality change, and the tube growth by adding C_2 dimers (Figure 2). In the former pathway, C atoms continuously adsorb on the pentagon edges followed by the pentagon edge reconstruction to form a hexagon edge, resulting in the configuration of other chiral caps (along the horizontal direction in Figure 2). Meanwhile, along the tube growth pathway, C_2 dimers are continuously added to the pentagon carbon edges. The caps will eventually evolve into the corresponding SWCNTs

TABLE 1. The Energies of the Various Caps at Different Spin Multiplicities: The Total Energy (a.u.), Zero-Point Vibrational Energy (ZPVE) (kcal/mol) at B3LYP/6-31G, and the Relative Energies (RE) (eV) (inclusion of the ZPVE)

	(5,5)			(6,5)			(7,5)			(8,5)			(9,5)		
multiplicity	total	ZPVE	RE	total	ZPVE	RE	total	ZPVE	RE	total	ZPVE	RE	total	ZPVE	RE
singlet	−1141.8848	105.37	**0.00**	−1637.2519	157.21	0.59	−1751.4093	166.63	1.55	−1865.5647	175.85	2.51	−1979.7366	185.05	3.36
triplet	−1141.8642	105.23	0.56	−1637.2735	156.86	**0.00**	−1751.4663	167.17	**0.00**	−1865.6577	177.07	**0.00**	−1979.8418	188.41	0.53
quintet	−1141.8434	105.08	1.13	−1637.2528	156.99	0.56	−1751.4465	166.05	0.53	−1865.6411	177.62	0.46	−1979.8611	187.73	**0.00**
septet													−1979.8325	187.63	0.78

(along the downward direction in Figure 2). Therefore, the C atom and C_2 dimer ratio and their concentrations are critical in such chirality and growth competition. The complete chirality change and tube growth pathways for (*n*,5) tubes where (*n* = 5, 6, 7, 8, and 9) are illustrated in Figure 2.

To uncover the reaction mechanism and elucidate the growth process in detail, we optimize the structures, intermediates, and transition states of cap (*n*,*m*) and calculate the activation energy of PESs. Here, we consider both singlet and triplet PESs of each reaction step as well as their intermediates and transition states. The complete PESs for all chirality changes induced by C atoms and the tube growth by adding C_2 dimers are given in Figures S1 and S2, respectively, in the Supporting Information.

To have a straightforward image of the aforementioned competitive reaction paths, we extract the initial steps of the reaction path for one type of (*n*,*m*) tubes ((6,5) tubes) among all the calculated results to illustrate the reaction PES details in Figure 3. In general, the path includes the following subsequent steps: (1) A single carbon atom is adsorbed on the pentagon edges of the (5,5) cap (^{1,3}Cap55-C). (2) A transition state (^{1,3}TsCap55-C/Int65) can be found between the ^{1,3}Cap55-C and newly formed (3) intermediate (^{1,3}Int65). (4) Then, the C_2 dimer is adsorbed on the pentagon edges of the intermediate ^{1,3}Int65 (^{1,3}Int65-C_2) to overcome (5) a transition state (^{1,3}TsInt65-C_2/Int65+C_2) barrier, existing between ^{1,3}Int65-C_2 and (^{1,3}Int65+C_2) intermediates. Finally, (6) when more C_2 dimers are incorporated into the growing cap, a (6,5) carbon nan-

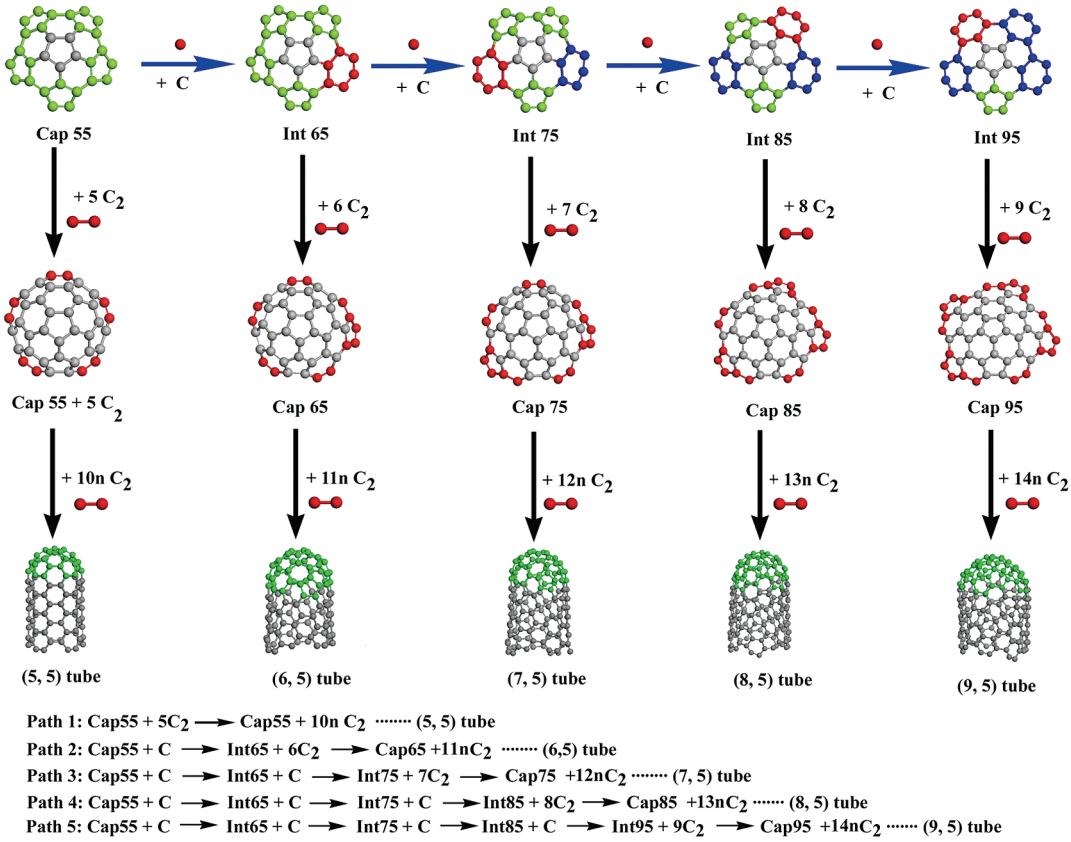

Figure 2. Schematic reaction paths of chirality change and nanotube growth *via* addition of C atoms or C_2 dimers for selected chiral caps. The vertical arrows indicate the cap growth processes leading to corresponding SWCNTs. The horizontal arrows represent the possible chirality change paths induced by individual C atoms.

TABLE 2. The Ground State Energies *per* C Atom of Different Caps and Their Relative Energy *per* C Atom with Respect to the Cap (5,5)

cap	chiral angle (deg)	energy/C atom (eV/C atom)	relative energies (eV)
(5,5)	30.00	−1035.59	0.00
(6,5)	27.00	−1035.95	−0.36
(7,5)	24.50	−1035.93	−0.34
(8,5)	22.41	−1035.91	−0.32
(9,5)	20.63	−1035.90	−0.31

otube is formed. To substantially support each step reaction in Figure 2, we have provided all the energy, structure details of the intermediates and transition states of the PESs in Tables S1, S2 and Figures S3, S4 in the Supporting Information.

Step 1 and step 4 in the PESs show that there are no energy barriers for either single C atom or C_2 dimer adsorbing on the pentagon edges of the caps, which is validated by the PES scans. In step 1, one single C atom tends to attach on the side of the pentagon edge (the C═C double bond), forming a trigon−pentagon pair intermediate. All (*n*,*m*) caps except the ^{3}Cap55-C cap under investigation have the similar C atom adsorption process as that in step 1 (see Figure S1 in the Supporting Information).

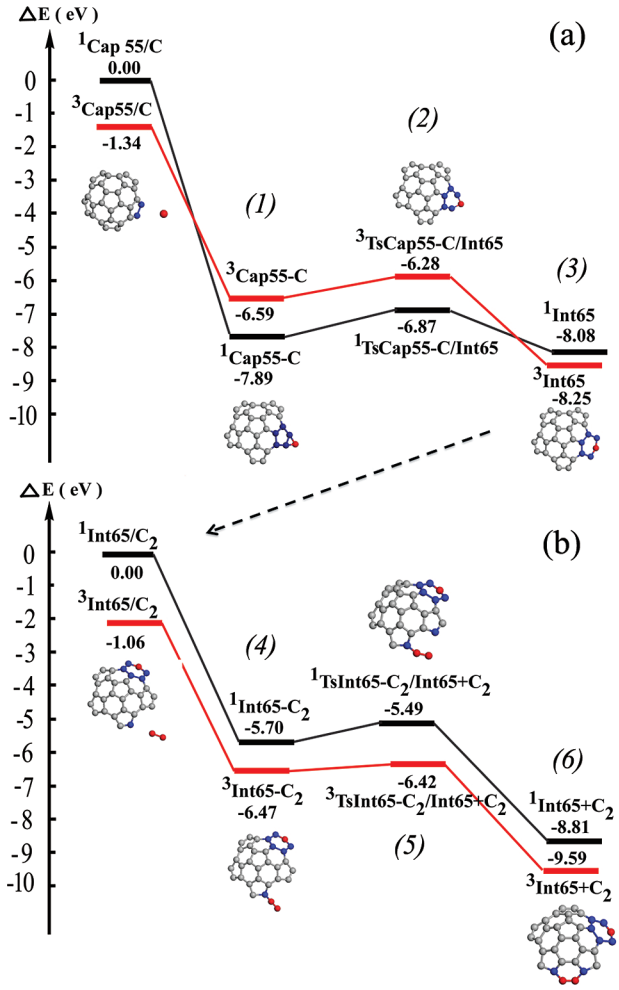

Figure 3. Schematic potential energy surfaces of singlet (black) and triplet (red) along the reaction "path 2" shown in Figure 2 at the B3LYP/6-31G level. (a) A single C atom induces the chirality change reaction. The relative energy of ^{1}Cap55/C is set to zero as a reference point for corresponding species. (b) The C_2 dimer addition growth reaction. The relative energy of ^{1}Int65/C_2 is set to zero as a reference point for corresponding species.

For all the caps, the adsorption energies of a single C atom at the singlet PES are higher than those at the triplet PES by 1.78−2.64 eV (Figure S1 in Supporting Information). Moreover, the adsorption energies increase with the cap diameters. The "Int95" has the largest adsorption energies of −9.56 and −7.11 eV at the singlet and triplet PESs, respectively (note that a large negative value indicates a more stable structure). This cap-diameter-dependent adsorption energy implies that it is easier for single C atoms to adsorb on larger diameter caps. In addition, as illustrated in step 4, a C_2 dimer prefers attaching to one carbon of the pentagon edge, and forms a C_2 side chain. The adsorption energies of C_2 dimers are −5.70 to −6.18 eV and −5.41 to −6.45 eV at singlet and triplet PESs (Figure S2 in the Supporting Information), respectively. The "Int95" has the largest adsorption energies of −11.89 (singlet) and −7.12 (triplet) eV. Overall, the adsorption energies of C_2 dimers are smaller than those of a single C atom by 0.72 to 2.15 eV.

Step 2 illustrates the transition state from the trigon-pentagon pair structure in step 1 to the hexagonal ring reaction intermediate in step 3. A total of 20 reaction intermediates for various (*n*,*m*) caps connected by 10 transition states were identified (Table S1 and Figure S3 in the Supporting Information). On the basis of the calculated energy barriers, it is easy to convert from a trigon−pentagon pair structure to a hexagonal ring reaction intermediate along the chirality change reaction path induced by adding single C atoms. Interestingly, the reaction energy barriers are different among various (*n*,*m*) structures (Figure S1 in Supporting Information). The energy barriers for ^{3}Int65-C and ^{3}Int75-C are almost zero at 0.02 and 0.03 eV, respectively; while the energy barriers for ^{3}Cap55-C, ^{3}Int85-C, and ^{3}Int95-C are 0.31, 0.56, and 0.97 eV, respectively. Furthermore, we also notice that the energy barriers in singlet PESs are slightly higher than those in their triplet PESs. For example, the energy barriers for ^{1}Int65-C and ^{1}Int75-C are 0.97 and 0.61 eV, respectively. Therefore, the relatively low energy barriers of those transition states suggest that the formation of the reaction intermediates with hexagonal ring structures is thermodynamically and kinetically favorable.

The transition state of C_2-induced tube growth is displayed as step 5. The growth is a close-ring reaction by incorporating C_2 side chains (the structure shown in step 4) into a new hexagonal ring. A total of 20 intermediates for various (*n*,*m*) caps connected by 10 transition states on the tube growth reaction pathways were identified (Figure S4 and Table S2 in

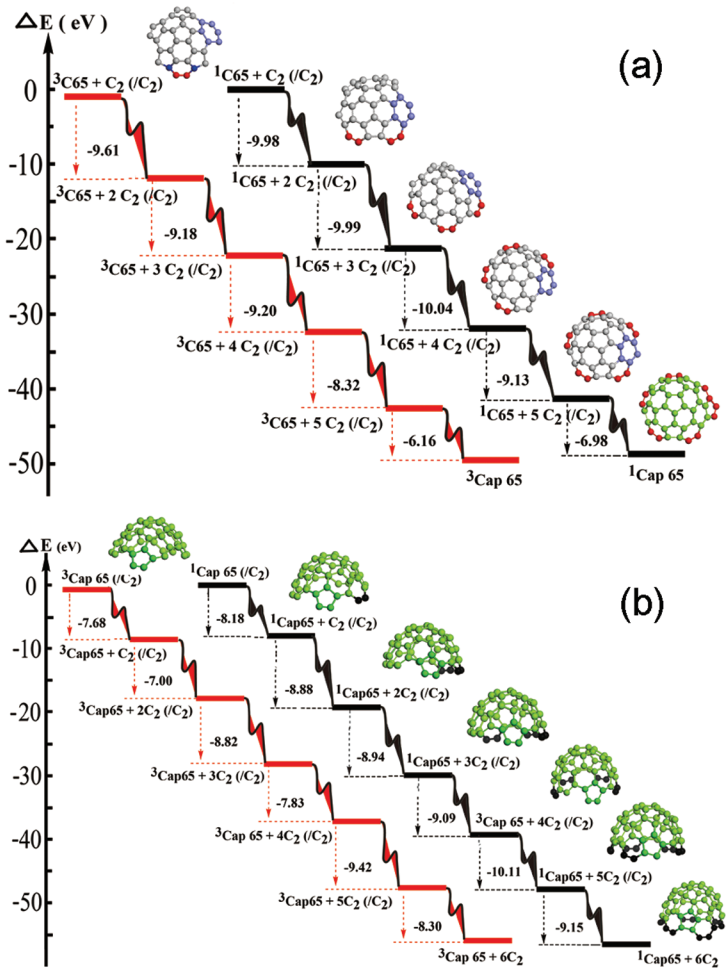

Figure 4. Schematic potential energy surfaces of the (6,5) cap formation and (6,5) tube growth processes along the reaction "Path 2" shown in Figure 2 at the B3LYP/6-31G level. Singlet (black) and triplet (red): (a) the (6,5) cap formation; (b) (6,5) tube growth by continuous addition of C_2 dimers to the edge of the (6,5) cap.

the Supporting Information). All energy barriers are lower than 0.42 eV (Figure S2 in the Supporting Information), implying an easy transformation from an adsorbed C_2 side chain to a new hexagonal ring. Similar to the chirality change reaction induced by single C atoms, the triplet PESs of tube growth reaction paths are more favorable than the singlet PESs.

Along the nanotube growth path, a near-armchair (6,5) cap can grow by continuously adding five C_2 dimers to the edge of ^{1,3}Int65+C_2 intermediate. The (6,5) cap formation process is illustrated in Figure 4a, following step 6 in Figure 3b. Each C_2 dimer addition step shown in Figure 4a has a similar adsorption feature as that in step 4 and close-ring reaction process as that in step 5. The addition would continue until a new hexagonal ring is formed. Similar energy changes of about −8.32 to −10.04 eV are found in the first five C_2 addition steps. Nevertheless, the last C_2 addition step has a lower energy than the first five steps at −6.98 (singlet) and −6.16 (triplet) eV. It could be due to the reconstruction of the carbon cap to form a new pentagonal ring in the last step. Once the (6,5) chiral cap is formed, this (6,5) cap is able to continuously grow into the corresponding (6,5) chiral tube by adding more C_2 dimers, as long as no defects are included in the growing carbon structure.

Figure 4b illustrates the sequential growth process of a (6,5) chiral tube by continuously adding six C_2 dimers to the edge of (6,5) cap. Each C_2 dimer addition step would repeat the similar process as the process illustrated in step 4 to step 6. The energy changes of adding C_2 in six steps at triplet are about −7.00 to −9.42 eV. Altogether, 11 C_2 (the number equals to $n + m$ for a specific (n,m) tube) are needed to grow one complete ring along the tube edge.

DISCUSSION

Our DFT calculations illustrate the detailed steps on how adding a single C atom induces the chirality change and how the incorporation of C_2 dimers grows the tube with the near-armchair chirality (n,5) caps where (n = 6, 7, 8, and 9) derived from a (5,5) cap. Some general information can be derived from these calculations: first, we show that the adsorption of C atom or C_2 dimer on growing carbon structures has no energy barrier. Second, the incorporation of adsorbed C atom or

C_2 dimer displays relatively low energy barriers. (Figures S1 and S2 in the Supporting Information). Third, the (*n*,*m*) nanotube growth will continue from specific (*n*,*m*) caps through C_2 dimer addition as long as no defects are introduced in the growing carbon structure.

Instead, there are several roles for catalysts in catalyzed SWCNT growth; note that the catalysts may include both metal and nonmetal nanoparticles. The first role is to facilitate the atomization of carbon precursor to produce single C atoms or C_2 dimers necessary for the tube growth with certain chirality evolution. This role is evident for metal nanoparticles, while further experimental evidence is still required to verify the same role for nonmetal nanoparticles. In some cases, plasma has been utilized to enhance the atomization of carbon precursor in chemical vapor deposition,[21,41] which results in SWCNT growth at low temperatures. Nevertheless, the thermal decomposition of carbon precursor gas can also occur at a high enough reaction temperature in the absence of catalyst, resulting in sufficient single C atoms or C_2 dimers for either chirality change or nanotube growth reaction. As a result, catalyst is not necessarily required for the atomization of carbon precursors.

The second role of catalyst is to prevent the spontaneous closure of growing nanotube free edges. Previous experimental results[11] and molecular dynamics simulations[17,22,25,26,42,43] have shown that the edge carbon atoms would move radically inward and arrange themselves in a structurally stable pentagonal configuration, resulting in a closed carbon cap. Inspecting all the singlet and triplet optimized structures found in this study (Figures S3 and S4 in Supporting Information), some defective tetragon configurations can be found on the large diameter intermediate caps, such as ^{1}Int85, ^{1,3}Int85-C, ^{1,3}Int95-C, ^{1,3}Int85-C_2, and ^{1,3}Int95-C_2 (highlighted in red color). Additions of dangling atoms/radicals (such as single C or C_2) on these carbon caps can generate high curvature strains on the edges. The high strains would lead to the shrinking of cap edges. With the addition of more C_2 dimers, the cap edge may eventually enclose and result in the formation of fullerene-like spherical carbon structures. Thus, the existence of nanoparticles may effectively prevent the cap enclosure of growing carbon structure in a fullerene-like manner and stabilize the dangling energy of cap/tube edges for the elongation of nanotubes at a fixed diameter. For this purpose, recent experimental findings[34−38] have demonstrated that metal catalyst nanoparticles may be replaced by various nonmetal nanoparticles.

The third role of catalyst nanoparticles is to assist the transformation of individual carbon species (such as C or C_2) into stable carbon caps, and to continuously deliver carbon species to the growing nanotubes. Our calculation results demonstrate that the direct adsorptions of C atom or C_2 dimer on growing carbon caps have no energy barrier. The incorporations of adsorbed C atom or C_2 dimer directly into growing carbon caps also display low energy barriers without the assistance of any catalysts. SWCNT growth and chirality change are thermodynamically and kinetically feasible under catalyst-free conditions. However, apart from activation energy barrier under catalyst-free conditions, catalyst nanoparticles are apparently influencing (*n*,*m*) selectivity toward specific carbon-cap structures.[3,4,11,20] The details of how do carbon species adsorb, diffuse, and organize on (or into) metal nanoparticles remain unclear. Moreover, whether or not nonmetal nanoparticles are involved in these processes also requires further verifications. We speculate that the influence of catalyst nanoparticles may be most critical for the initial carbon cap formation; further research is ongoing on this topic in our lab.

From the aspect of chiral-selective SWCNT synthesis, the relatively low energy barriers (all are lower than 1.02 eV) among different reaction pathways bring challenges in manipulating the selectivity toward a particular (*n*,*m*) tube. In particularly, the addition of single C atoms on larger diameter caps is more energetically favorable, which may result in more chirality changes. This suggests that it would be more feasible to achieve chirality control on small diameter SWCNTs over larger diameter ones. Our calculation results show that the energy barriers of nanotube growth reactions for (6,5) ("Path 2" in Figure 2) and (7,5) tubes ("Path 3") are smaller than those of (8,5) ("Path 4") and (9,5) ("Path 5"). We predict that the chiral-selective growth of SWCNTs is more likely to be achieved on (*n*,*m*) species with low energy barriers such as (6,5) and (7,5).

Considering the competition between the chirality change pathway and the tube growth pathway, because the initial adsorptions of either a single C atom or C_2 dimer on the pentagon edge of the carbon caps show no energy barriers, the concentrations of C atoms and C_2 dimers in the experimental environment would thus also play a strong role in the chiral-selective SWCNT synthesis. The existence of abundant single C atoms would facilitate the chirality change reaction path; while the presence of C_2 dimers can push forward the nanotube growth. The concentrations of C or C_2 species can be changed by many experimental reaction parameters, such as temperature, chemistry of carbon precursors, pressure, and plasma power,[3−12] and may help explain the preferential growth of specific chiralities in previous experiments.

A recent study has investigated the time dependent concentration changes of C, C_2, and C_3 species during the decomposition of acetylene.[44] It shows that the C_2 and C_3 species are absent for the first 1 ms; both the C_2 and C_3 species appear in considerable amount in subsequent 10 ms; the C_2 and C_3 amounts increase proportionally with reaction time later on.[44] We propose a possible strategy for chirality selection would be delivering the C atoms at the early stage of SWCNT growth.

Once the desired chiral caps are formed, it would be more efficient to promote the C_2 dimer addition growth reaction with the increase of C_2 dimer amount in reaction environment. Therefore, the control of reaction conditions in a short time scale would be critical to achieve the (*n*,*m*) selective SWCNT growth.

CONCLUSION

We have presented a growth and chirality change mechanism for selected chiral nanotubes *via* precise PES survey using DFT calculations. The adsorptions of C atom or C_2 dimer on growing carbon structures show no energy barrier. The armchair (5,5) cap can evolve to near-armchair (*n*,5) where (n = 6, 7, 8, and 9) caps by changing its chirality and increasing its diameter. Both the single C induced chirality change and C_2 addition nanotube growth reaction processes have low energy barriers. The processes are more favorable *via* the triplet PES than the singlet PES. SWCNT growth and chirality change are thermodynamically and kinetically feasible under catalyst-free growth conditions. In addition to assist the initial carbon cap nucleation, nanoparticles may play roles in SWCNT growth by preventing the enclosure of the growing carbon structure in a fullerene-like manner and assist the elongation growth of nanotubes at a fixed diameter. Chiral-selective growth is additionally possible if the concentrations of single C atoms and C_2 dimers in the experimental environment can be precisely managed at different reaction stages.

MODELS AND METHODOLOGY

The carbon cap structures are given in Figure 1, and the calculations were carried out using Gaussian 03 program package.[45] The geometries of these chiral caps, intermediates, and interconversion transition states were fully optimized at B3LYP/6-31G level followed by harmonic vibrational frequency calculations to confirm their stationary points. Meanwhile, we performed intrinsic reaction coordinate (IRC) calculations at B3LYP/6-31G level to confirm whether the transition states are connected to the right reaction intermediates or not.[46] Zero-point vibrational energies (ZPVE) were included in all given energies.

Each cap consists of six pentagons and a number of hexagons, similar as a half fullerene.[14,39] The matching cap of each specific chiral SWCNT can be uniquely constructed by arranging the position of these six pentagons and some hexagons according to the isolated pentagon rule;[39,40] (5,5) and (6,5) have only one cap obeying the isolated pentagon rule. Cap (5,5) can be constructed by adding five additional pentagons along the directions of arrows. Other chiral caps of (6,5), (7,5), (8,5), and (9,5) are built from the (5,5) cap by moving one or several pentagons outward along the arrows using the graphical modeling technique.[40] These caps can grow into the corresponding SWCNTs with the specific (*n*,*m*) structure *via* the continuous addition of C_2 dimers, as long as no defects are included in the structure.[13−16]

Acknowledgment. We are grateful to AcRF tier 2 (ARC 13/07) from Ministry of Education, Singapore, and CRP (NRF-CRP2-2007-02) from National Research Foundation, Singapore, for financial support. The authors thank reviewers for helpful comments to improve this work.

Supporting Information Available: The complete potential energy surfaces for both single C atom induced chirality change reactions and C_2 dimer addition growth reactions on different chiral caps; the energies and optimized geometries of singlet and triplet reaction intermediates and transition states. This material is available free of charge *via* the Internet at http://pubs.acs.org.

REFERENCES AND NOTES

1. Jorio, A., Dresselhaus, G., Dresselhaus, M. S., Eds. *Carbon Nanotubes, Advanced Topics in the Synthesis, Structure, Properties and Applications*; Springer: Berlin, 2008; p 735.
2. Joselevich, E.; Dai, H.; Liu, J.; Hata, K.; Windle, A. H. Carbon Nanotube Synthesis and Organization. In *Carbon Nanotubes, Advanced Topics in the Synthesis, Structure, Properties and Applications*; Springer: Berlin, 2008; Vol. 111, pp 101−164.
3. Bachilo, S. M.; Balzano, L.; Herrera, J. E.; Pompeo, F.; Resasco, D. E.; Weisman, R. B. Narrow (*n*,*m*)-Distribution of Single-Walled Carbon Nanotubes Grown Using a Solid Supported Catalyst. *J. Am. Chem. Soc.* **2003**, *125*, 11186–11187.
4. Miyauchi, Y.; Chiashi, S.; Murakami, Y.; Hayashida, Y.; Maruyama, S. Fluorescence Spectroscopy of Single-Walled Carbon Nanotubes Synthesized from Alcohol. *Chem. Phys. Lett.* **2004**, *387*, 198–203.
5. Lolli, G.; Zhang, L. A.; Balzano, L.; Sakulchaicharoen, N.; Tan, Y. Q.; Resasco, D. E. Tailoring (*n*,*m*) Structure of Single-Walled Carbon Nanotubes by Modifying Reaction Conditions and the Nature of the Support of CoMo Catalysts. *J. Phys. Chem. B* **2006**, *110*, 2108–2115.
6. Smalley, R. E.; Li, Y. B.; Moore, V. C.; Price, B. K.; Colorado, R.; Schmidt, H. K.; Hauge, R. H.; Barron, A. R.; Tour, J. M. Single Wall Carbon Nanotube Amplification: *En route* to a Type-Specific Growth Mechanism. *J. Am. Chem. Soc.* **2006**, *128*, 15824–15829.
7. Wang, B.; Poa, C. H. P.; Wei, L.; Li, L.-J.; Yang, Y.; Chen, Y. (*n*,*m*) Selectivity of Single-Walled Carbon Nanotubes by Different Carbon Precursors on Co−Mo Catalysts. *J. Am. Chem. Soc.* **2007**, *129*, 9014–9019.
8. Li, X.; Tu, X.; Zaric, S.; Welsher, K.; Seo, W. S.; Zhao, W.; Dai, H. Selective Synthesis Combined with Chemical Separation of Single-Walled Carbon Nanotubes for Chirality Selection. *J. Am. Chem. Soc.* **2007**, *129*, 15770–15771.
9. Wang, B.; Wei, L.; Yao, L.; Li, L.-J.; Yang, Y.; Chen, Y. Pressure-Induced Single-Walled Carbon Nanotube (*n*,*m*) Selectivity on Co−Mo Catalysts. *J. Phys. Chem. C* **2007**, *111*, 14612–14616.
10. Ishigami, N.; Ago, H.; Imamoto, K.; Tsuji, M.; Iakoubovskii, K.; Minami, N. Crystal Plane Dependent Growth of Aligned Single-Walled Carbon Nanotubes on Sapphire. *J. Am. Chem. Soc.* **2008**, *130*, 9918–9924.
11. Jin, C.; Suenaga, K.; Iijima, S. How Does a Carbon Nanotube Grow? An *in Situ* Investigation on the Cap Evolution. *ACS Nano* **2008**, *2*, 1275–1279.
12. Wang, B.; Yang, Y.; Li, L. J.; Chen, Y. Effect of Different Catalyst Supports on the (*n*,*m*) Selective Growth of Single-Walled Carbon Nanotube from Co−Mo Catalyst. *J. Mater. Sci.* **2009**, *44*, 3285–3295.
13. Reich, S.; Li, L.; Robertson, J. Structure and Formation Energy of Carbon Nanotube Caps. *Phys. Rev. B: Condens. Matter* **2005**, *72*, 165423.
14. Reich, S.; Li, L.; Robertson, J. Control the Chirality of Carbon Nanotubes by Epitaxial Growth. *Chem. Phys. Lett.* **2006**, *421*, 469–472.
15. Zhao, J.; Balbuena, P. B. Effect of Nanotube Cap on the Aromaticity of Single-Wall Carbon Nanotubes. *J. Phys. Chem. C* **2008**, *112*, 13175–13180.

16. Zhao, J.; Balbuena, P. B. Effect of Nanotube Length on the Aromaticity of Single-Wall Carbon Nanotubes. *J. Phys. Chem. C* **2008**, *112*, 3482–3488.
17. Gomez-Gualdron, D. A.; Balbuena, P. B. The Role of Cap Chirality in the Mechanism of Growth of Single-Wall Carbon Nanotubes. *Nanotechnology* **2008**, *19*, 485604.
18. Gomez-Gualdron, D. A.; Balbuena, P. B. Growth of Chiral Single-Walled Carbon Nanotube Caps in the Presence of a Cobalt Cluster. *Nanotechnology* **2009**, *20*, 215601.
19. Gomez-Gualdron, D. A.; Balbuena, P. B. Effect of Metal Cluster-Cap Interactions on the Catalyzed Growth of Single-Wall Carbon Nanotubes. *J. Phys. Chem. C* **2009**, *113*, 698–709.
20. Chiang, W.-H.; Sankaran, R. M. Linking Catalyst Composition to Chirality Distributions of As-Grown Single-Walled Carbon Nanotubes by Tuning Ni_xFe_{1-x} Nanoparticles. *Nat. Mater.* **2009**, *8*, 882–886.
21. Li, Y. M.; Peng, S.; Mann, D.; Cao, J.; Tu, R.; Cho, K. J.; Dai, H. J. On the Origin of Preferential Growth of Semiconducting Single-Walled Carbon Nanotubes. *J. Phys. Chem. B* **2005**, *109*, 6968–6971.
22. Ding, F.; Larsson, P.; Larsson, J. A.; Ahuja, R.; Duan, H. M.; Rosen, A.; Bolton, K. The Importance of Strong Carbon−Metal Adhesion for Catalytic Nucleation of Single-Walled Carbon Nanotubes. *Nano Lett.* **2008**, *8*, 463–468.
23. Hofmann, S.; Sharma, R.; Ducati, C.; Du, G.; Mattevi, C.; Cepek, C.; Cantoro, M.; Pisana, S.; Parvez, A.; Cervantes-Sodi, F.; *et al. In Situ* Observations of Catalyst Dynamics During Surface-Bound Carbon Nanotube Nucleation. *Nano Lett.* **2007**, *7*, 602–608.
24. Yoshida, H.; Takeda, S.; Uchiyama, T.; Kohno, H.; Homma, Y. Atomic-Scale *in-Situ* Observation of Carbon Nanotube Growth from Solid State Iron Carbide Nanoparticles. *Nano Lett.* **2008**, *8*, 2082–2086.
25. Ohta, Y.; Okamoto, Y.; Irle, S.; Morokuma, K. Rapid Growth of a Single-Walled Carbon Nanotube on an Iron Cluster: Density-Functional Tight-Binding Molecular Dynamics Simulations. *ACS Nano* **2008**, *2*, 1437–1444.
26. Ohta, Y.; Okamoto, Y.; Page, A. J.; Irle, S.; Morokuma, K. Quantum Chemical Molecular Dynamics Simulation of Single-Walled Carbon Nanotube Cap Nucleation on an Iron Particle. *ACS Nano* **2009**, *3*, 3413–3420.
27. Amara, H.; Bichara, C.; Ducastelle, F. Understanding the Nucleation Mechanisms of Carbon Nanotubes in Catalytic Chemical Vapor Deposition. *Phys. Rev. Lett.* **2008**, *100*, 056105.
28. Harris, P. J. F. Solid State Growth Mechanisms for Carbon Nanotubes. *Carbon* **2007**, *45*, 229–239.
29. Hofmann, S.; Csanyi, G.; Ferrari, A. C.; Payne, M. C.; Robertson, J. Surface Diffusion: The Low Activation Energy Path for Nanotube Growth. *Phys. Rev. Lett.* **2005**, *95*, 036101.
30. Zhu, W. M.; Rosen, A.; Bolton, K. Changes in Single-Walled Carbon Nanotube Chirality During Growth and Regrowth. *J. Chem. Phys.* **2008**, *128*, 124708.
31. Zhu, W. M.; Duan, H. M.; Bolton, K. Diameter and Chirality Changes of Single-Walled Carbon Nanotubes During Growth: An *ab-Initio* Study. *J. Nanosci. Nanotechnol.* **2009**, *9*, 1222–1225.
32. Ding, F.; Harutyunyan, A. R.; Yakobson, B. I. Dislocation Theory of Chirality-Controlled Nanotube Growth. *Proc. Nat. Acad. Sci. U.S.A.* **2009**, *106*, 2506–2509.
33. Marchand, M.; Journet, C.; Guillot, D.; Benoit, J. M.; Yakobson, B. I.; Purcell, S. T. Growing a Carbon Nanotube Atom by Atom: "And Yet It Does Turn". *Nano Lett.* **2009**, *9*, 2961–2966.
34. Huang, S. M.; Cai, Q. R.; Chen, J. Y.; Qian, Y.; Zhang, L. J. Metal-Catalyst-Free Growth of Single-Walled Carbon Nanotubes on Substrates. *J. Am. Chem. Soc.* **2009**, *131*, 2094–2095.
35. Liu, B.; Ren, W.; Gao, L.; Li, S.; Pei, S.; Liu, C.; Jiang, C.; Cheng, H.-M. Metal-Catalyst-Free Growth of Single-Walled Carbon Nanotubes. *J. Am. Chem. Soc.* **2009**, *131*, 2082–2083.
36. Hirsch, A. Growth of Single-Walled Carbon Nanotubes without a Metal Catalyst—A Surprising Discovery. *Angew. Chem., Int. Ed.* **2009**, *48*, 5403–5404.
37. Steiner, S. A.; Baumann, T. F.; Bayer, B. C.; Blume, R.; Worsley, M. A.; MoberlyChan, W. J.; Shaw, E. L.; Schlogl, R.; Hart, A. J.; Hofmann, S.; Wardle, B. L. Nanoscale Zirconia as a Nonmetallic Catalyst for Graphitization of Carbon and Growth of Single- and Multiwall Carbon Nanotubes. *J. Am. Chem. Soc.* **2009**, *131*, 12144–12154.
38. Takagi, D.; Kobayashi, Y.; Homma, Y. Carbon Nanotube Growth from Diamond. *J. Am. Chem. Soc.* **2009**, *131*, 6922–6923.
39. Brinkmann, G.; Fowler, P. W.; Manolopoulos, D. E.; Palser, A. H. R. A Census of Nanotube Caps. *Chem. Phys. Lett.* **1999**, *315*, 335–347.
40. Lair, S. L.; Herndon, W. C.; Murr, L. E.; Quinones, S. A. End Cap Nucleation of Carbon Nanotubes. *Carbon* **2006**, *44*, 447–455.
41. Li, Y. M.; Mann, D.; Rolandi, M.; Kim, W.; Ural, A.; Hung, S.; Javey, A.; Cao, J.; Wang, D. W.; Yenilmez, E.; *et al.* Preferential Growth of Semiconducting Single-Walled Carbon Nanotubes by a Plasma Enhanced CVD Method. *Nano Lett.* **2004**, *4*, 317–321.
42. Hossain, M. Z. Structural Instability of Single Wall Carbon Nanotube Edges from First Principles. *Appl. Phys. Lett.* **2009**, *95*, 3250159.
43. Ohta, Y.; Okamoto, Y.; Irle, S.; Morokuma, K. Temperature Dependence of Iron-Catalyzed Continued Single-Walled Carbon Nanotube Growth Rates: Density Functional Tight-Binding Molecular Dynamics Simulations. *J. Phys. Chem. C* **2009**, *113*, 159–169.
44. Moors, M.; Amara, H.; de Bocarme, T. V.; Bichara, C.; Ducastelle, F.; Kruse, N.; Charlier, J. C. Early Stages in the Nucleation Process of Carbon Nanotubes. *ACS Nano* **2009**, *3*, 511–516.
45. Frisch, M. J.; Trucks, G. W.; Schlegel, H. B.; Scuseria, G. E.; Robb, M. A.; Cheeseman, J. R.; Montgomery, J., J.; Vreven, A. T.; Kudin, K. N.; Burant, J. C.; *et al. Gaussian 03*, revision C.01; Gaussian, Inc.: Wallingford, CT, 2004.
46. Gonzalez, C.; Schlegel, H. B. An Improved Algorithm for Reaction-Path Following. *J. Chem. Phys.* **1989**, *90*, 2154–2161.